

# Stabilities and Energetics of Inorganic Benzene Isomers: Prismanes

Nikita Matsunaga and Mark S. Gordon\*

Contribution from the Department of Chemistry, Iowa State University, Ames, Iowa 50011-3111

Received March 28, 1994<sup>Ⓢ</sup>

**Abstract:** *Ab initio* calculations of inorganic prismanes, with the formula (XH–YH)<sub>3</sub>, where X = B, Al, and Ga and Y = N, P, and As, as well as X or Y = C, Si, and Ge, were carried out. Energetics of these species are compared with those of the planar benzene analog and chair/boat conformers. The prismane and planar structures containing first period elements (B, C, and N) are all stable (*i.e.* minima on the potential energy surfaces). Chair and boat conformers are potential energy minima only in compounds containing second or third period elements. For those species with a first period element in the 1, 3, 5 positions, the planar benzene-like structure is the global minimum; otherwise, the planar structure is not a minimum. The lowest minimum found is the prismane arrangement for Si<sub>6</sub>H<sub>6</sub> and Ge<sub>6</sub>H<sub>6</sub> and the chair structure for Si<sub>3</sub>Ge<sub>3</sub>H<sub>6</sub>. Other molecules have distorted minima.

## Introduction

More than 20 years ago, Woodward and Hoffman<sup>1</sup> observed that, "...the excess energy of the prismane molecule must have the aspect of an angry tiger unable to break out of a paper cage." Subsequently, these authors analyzed the nature of the bonding in prismane, and demonstrated that the above is not at all true: Upon breaking three of the  $\sigma$  bonds in prismane the resulting  $\pi$  orbital is an antibonding orbital of benzene, thus the isomerization is a symmetry forbidden reaction. This results in a high-energy transition state, and hence prismane is kinetically stable.

There are a number of valence isomers of benzene, including Dewar benzene, prismane, and benzvalene, that can be synthesized.<sup>2</sup> In particular, the photochemical conversion of benzene into these isomers has been known for some time. For example, when substituted benzene is irradiated with UV light ( $\lambda = 254$  nm), it is converted into prismane and Dewar benzene.<sup>2f</sup> Other photochemical paths have been established to convert Dewar benzene to prismane and benzene and to convert prismane to Dewar benzene and benzene.<sup>2k</sup>

The first heavier group IV containing organometallic benzene analog, silatoluene, was isolated by Barton and co-workers.<sup>3</sup> Silabenzene and 1,4-disilabenzene were isolated later in a low-temperature argon matrix.<sup>4</sup> These studies have spawned several theoretical investigations on compounds that are potentially

aromatic. Singly substituted silabenzene,<sup>5b</sup> disilabenzene,<sup>5a</sup> and germabenzene<sup>5b</sup> have been studied by this group. The only other species investigated theoretically was hexasilabenzene.<sup>6</sup> Though the structure of 1,3,5-trisilabenzene is yet to be determined, there is recent experimental evidence that a gas-phase dehydrogenation reaction of 1,3,5-trisilacyclohexane with a Cp-transition metal (Fe, Co, or Ni) cationic complex forms a [Cp–M]<sup>+</sup>–1,3,5-trisilabenzene complex.<sup>7</sup>

Borazine had been the only inorganic isomer of benzene known for quite some time.<sup>8</sup> With increasing attention paid to exotic species, three group III–group V benzene analogs have recently been synthesized by Power *et al.*<sup>9,10</sup> These are B–P ([MesBPPPh]<sub>3</sub>), Al–N ([MeAlN(2,6-*i*-Pr<sub>2</sub>C<sub>6</sub>H<sub>3</sub>)<sub>3</sub>]), and Ga–P ([{(2,4,6-Ph<sub>3</sub>C<sub>6</sub>H<sub>2</sub>)GaP(cyclo-C<sub>6</sub>H<sub>11</sub>)<sub>3</sub>}]<sub>3</sub>) systems containing alternating group III and group V elements. They have been isolated with large substituents to stabilize the ring. NMR evidence together with X-ray crystallographic data suggest that the B–P and the Al–N species are planar, and that there is some delocalization of the lone pair from the group V elements into the empty p-orbitals of neighboring group III elements.<sup>9c,d</sup> In the case of the Ga–P system the ring is not planar; it assumes a slightly twisted boat conformation.<sup>10</sup> Fink and Richards<sup>11</sup> have calculated the "resonance energies" of the planar B–N, B–P, and Al–N systems by using homodesmotic reactions<sup>12</sup> and have concluded that the resonance energy of the B–P system is about the same as that of borazine.

<sup>Ⓢ</sup> Abstract published in *Advance ACS Abstracts*, November 1, 1994.

(1) Woodward, R. B.; Hoffmann, R. *The Conservation of Orbital Symmetry*; Verlag Chemie GmbH: Weinheim/Bergstr, 1970; p 107–112.

(2) (a) van Tamelen, E. E.; Pappas, S. P. *J. Am. Chem. Soc.* **1962**, *84*, 3789. (b) van Tamelen, E. E.; Pappas, S. P. *J. Am. Chem. Soc.* **1963**, *85*, 3297. (c) Viehe, H. G.; Merenyi, D. R.; Oth, J. F. M.; Senders, J. R.; Vahange, P. *Angew. Chem., Int. Ed. Engl.* **1964**, *3*, 755. (d) van Tamelen, E. E. *Angew. Chem., Int. Ed. Engl.* **1965**, *4*, 738. (e) Viehe, H. G. *Angew. Chem., Int. Ed. Engl.* **1965**, *4*, 746. (f) Wilzbach, K. E.; Kaplan, L. *J. Am. Chem. Soc.* **1965**, *87*, 4004. (g) Bryce-Smith, D.; Gilbert, A.; Robinson, D. A. *Angew. Chem., Int. Ed. Engl.* **1971**, *10*, 745. (h) van Tamelen, E. E.; Pappas, S. P.; Kirk, K. L. *J. Am. Chem. Soc.* **1971**, *93*, 6092. (i) Breslow, R.; Napierski, J.; Schmidt, A. H. *J. Am. Chem. Soc.* **1972**, *94*, 5906. (j) Katz, T. J.; Acton, N. *J. Am. Chem. Soc.* **1973**, *95*, 2738. (k) Turro, N. J.; Ramamurthy, V.; Katz, T. J. *Nouv. J. Chim.* **1977**, *1*, 363. (l) Potgieter, J. H. *J. Chem. Educ.* **1991**, *68*, 280.

(3) (a) Barton, T. J.; Banasiak, D. *J. Am. Chem. Soc.* **1977**, *99*, 5199. (b) Barton, T. J.; Burns, G. T. *J. Am. Chem. Soc.* **1978**, *100*, 5246. (c) Barton, T. J.; Vuper, M. *J. Am. Chem. Soc.* **1981**, *103*, 6788.

(4) Maier, G.; Mihm, G.; Reisenauer, H. P. *Angew. Chem., Int. Ed. Engl.* **1980**, *19*, 52.

(5) (a) Baldrige, K. K.; Gordon, M. S. *J. Organomet. Chem.* **1984**, *271*, 369. (b) Baldrige, K. K.; Gordon, M. S. *J. Am. Chem. Soc.* **1988**, *110*, 4204.

(6) (a) Nagase, S.; Kudo, T.; Aoki, M. *J. Chem. Soc. Chem. Commun.* **1985**, 1121. (b) Sax, A.; Janoschek, R. *Angew. Chem., Int. Ed. Engl.* **1986**, *25*, 651. (c) Clabo, D. A., Jr.; Schaefer, H. F. *J. Chem. Phys.* **1986**, *84*, 1664. (d) Nagase, S.; Teramae, H.; Kudo, T. *J. Chem. Phys.* **1987**, *86*, 4513. (e) Nagase, S. *Angew. Chem., Int. Ed. Engl.* **1989**, *28*, 329. (f) Slanina, Z. *Chem. Phys. Lett.* **1989**, *161*, 175.

(7) Bjarnason, A.; Arnason, I. *Angew. Chem., Int. Ed. Engl.* **1992**, *31*, 1633.

(8) Stock, A.; Pohland, E. *Dtsch. Chem. Ges.* **1926**, *59*, 2215.

(9) (a) Dias, H. V. R.; Power, P. P. *Angew. Chem., Int. Ed. Engl.* **1987**, *26*, 1270. (b) Dias, H. V. R.; Power, P. P. *J. Am. Chem. Soc.* **1989**, *111*, 144. (c) Power, P. P. *Angew. Chem., Int. Ed. Engl.* **1990**, *29*, 449. (d) Waggoner, K. M.; Hope, H.; Power, P. P. *Angew. Chem., Int. Ed. Engl.* **1988**, *27*, 1699. (e) Waggoner, K. M.; Power, P. P. *J. Am. Chem. Soc.* **1991**, *113*, 3385. (f) Hope, H.; Pestana, D. C.; Power, P. P. *Angew. Chem., Int. Ed. Engl.* **1990**, *29*, 449.

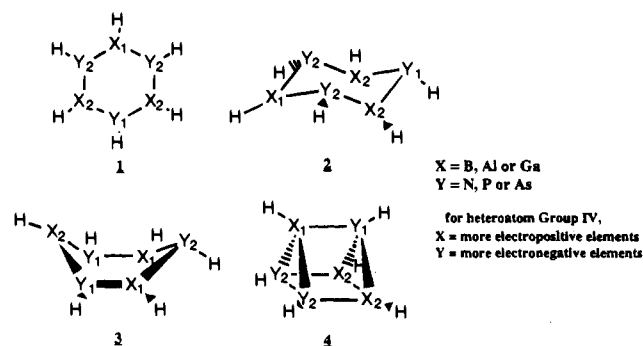
(10) Hope, H.; Pestana, D. C.; Power, P. P. *Angew. Chem., Int. Ed. Engl.* **1991**, *30*, 691.

(11) Fink, W. H.; Richards, J. C. *J. Am. Chem. Soc.* **1991**, *113*, 3393.

In our previous paper<sup>13</sup> on this subject we explored the possible existence of inorganic benzenes and the extent to which the  $\pi$ -electrons are delocalized. The species investigated included 1,3,5/2,4,6 combinations of the group III (B, Al, Ga)—group V (N, P, As) elements and group IV  $E_6H_6$  ( $E = C, Si,$  and  $Ge$ ). In that paper only planar species were considered, and it was found that only those compounds with carbon or nitrogen in alternating positions correspond to minima on their potential energy surfaces (PES). The remaining species have at least one imaginary frequency corresponding to an out-of-plane motion. Those that are not minima are either transition states or higher-order saddle points that lead to boat and/or chair conformations.

There are only a handful of studies on the subject of geometrical isomers of inorganic benzenes. Even fewer studies are available in the literature on the subject of prismane analogs.<sup>14–16</sup> Hexagermaprismane with six bis(trimethylsilyl)-methyl substituents was the first inorganic analog of prismane reported by Sakurai *et al.*<sup>14</sup> Recently the same group has reported the synthesis of 2,6-diisopropylphenyl-substituted hexasilaprismane, as well as hexagermaprismane.<sup>15</sup> Although they belong to the same group, the behavior of silicon is markedly different from that of carbon. For example,  $C_6H_6$  in a prismane framework is stable (a minimum on the PES), but it is one of the highest energy isomers. However, theoretical calculations predict that the silicon analog of benzene is easily distorted to become a chair conformation,<sup>6c</sup> and the prismane analog appears to be the global minimum. The prismane  $Si_6H_6$  structure is estimated to be about 10 kcal/mol<sup>6a,b</sup> more stable than the planar geometry with an RHF wave function using an effective core potential basis set.

In this paper, we focus our attention on the structures and the energetics of prismane analogs (**4**) relative to the benzene-like planar structure (**1**) and “chair” (**2**) and “boat” (**3**) conformers. The species considered here have the general



formula  $X_3Y_3H_6$  (with X and Y alternating in a ring), where X and Y are chosen from group III (B, Al, and Ga), group IV (C, Si, Ge), and group V (N, P, and As), such that each compound is valence isoelectronic with prismane. Also, the nature of the bonding in **4** is analyzed in order to determine a correlation

(12) (a) A homodesmotic reaction is a reaction that conserves the type and number of bonds to calculate resonance energy. For example, the resonance energy of benzene can be calculated from the following:  $3CH_2=CHCH=CH_2 \rightarrow C_6H_6 + 3CH_2=CH_2$ . (b) George, P.; Trachtman, M.; Bock, C. W.; Brett, A. M. *Theor. Chim. Acta* **1975**, *38*, 121. (c) George, P.; Trachtman, M.; Bock, C. W.; Brett, A. M. *J. Chem. Soc., Perkin Trans. 1976*, *2*, 1222. (d) George, P.; Trachtman, M.; Bock, C. W.; Brett, A. M. *Tetrahedron* **1976**, *32*, 1357. (e) See for example ref 5.

(13) Matsunaga, N.; Cundari, T. R.; Schmidt, M. W.; Gordon, M. S. *Theor. Chim. Acta* **1992**, *83*, 57.

(14) Sekiguchi, A.; Kubota, C.; Sakurai, H. *Angew. Chem., Int. Ed. Engl.* **1989**, *28*, 55.

(15) Sekiguchi, A.; Yatabe, T.; Kubota, C.; Sakurai, H. *J. Am. Chem. Soc.* **1993**, *115*, 5853.

between bonding characteristics and the stabilities as a function of X and Y.

## Computational Approach

All calculations described here were performed with the GAMESS *ab initio* quantum chemistry program package.<sup>16</sup> These extensive calculations were facilitated by the recent implementation of a parallel version of the code for use on a CM5 and an iPSC/860. The initial calculations were carried out at the restricted Hartree–Fock (RHF) level of theory using the Stevens–Basch–Krauss–Jasien (SBKJ) effective core potentials (ECP) and basis sets<sup>17</sup> for all heavy atoms and the -31G basis<sup>18a</sup> for hydrogen. The full core potential, which projects out all 3d electrons, and the corresponding basis set, was used for gallium atom. These bases are augmented with d-polarization functions<sup>19</sup> for all heavy atoms.

Geometries of **4** were optimized in  $C_s$  symmetry for the heteronuclear prismanes ( $X \neq Y$ ) and in  $D_{3h}$  symmetry for the homonuclear prismanes. Geometries of **2** and **3** were optimized in  $C_{3v}$  and  $C_s$  symmetries, respectively, for the heteronuclear species, and in  $D_{3d}$  and  $C_{2v}$  for the homonuclear species. Geometries predicted using the SBKJ effective core potentials and associated basis sets (these bases are referred to below as basis-A) have been found to be in good agreement with experimental results for both main group<sup>13,20</sup> and transition metal<sup>21</sup> compounds. The matrices of energy second derivatives (hessians) were calculated numerically from analytically determined gradients, in order to verify the given geometry is a minimum (all eigenvalues of hessian are positive) or a transition state (the hessian has one and only one negative eigenvalue).

Structures **1** and **4** of three species (Ge–C, Ge–Ge, and B–N) were optimized with the MP2/basis-A level of theory using Gaussian 92<sup>22</sup> in order to examine the effect of correlated wave functions on geometries and relative energies. These three species were chosen because the largest differences between the RHF and MP2 energies were observed for them using geometries obtained with the RHF/basis-A level of theory.

At each stationary point found with the RHF/basis-A level of theory, RHF and MP2 energies were recalculated with two all-electron basis sets: Basis-B consists of 6-31G(d)<sup>18b–c</sup> for the first and second period elements and the (14s12p6d) primitive gaussian set contracted to [6s5p2d]<sup>24</sup> for the third period elements. Basis-C consists of 6-311G-(d,p)<sup>23</sup> for the first and second period elements and the [9s7p3d] contraction<sup>24</sup> using the (14s12p6d) primitive set for the third period elements. The correlation energy was calculated by means of second-

(16) (a) Schmidt, M. W.; Baldrige, K. K.; Boatz, J. A.; Elbert, S. T.; Gordon, M. S.; Jensen, J. H.; Koseki, S.; Matsunaga, N.; Nguyen, K. A.; Su, S.; Windus, T. L.; Dupuis, M.; Montgomery, J. A., Jr. *J. Comput. Chem.* **1993**, *14*, 1347. (b) Contact Mike Schmidt at mike@si.fi.ameslab.gov concerning this program.

(17) (a) B–O, Al–S: Stevens, W. J.; Basch, H.; Krauss, M. *J. Chem. Phys.* **1984**, *81*, 6026. (b) Zn–Ge: Stevens, W. J.; Krauss, M.; Jasien, P. *G. Can. J. Chem.* **1992**, *70*, 612.

(18) (a) Ditchfield, R.; Hehre, W. J.; Pople, J. A. *J. Chem. Phys.* **1971**, *54*, 724. (b) Dill, J. D.; Pople, J. A. *J. Chem. Phys.* **1975**, *62*, 2921. (c) Hehre, W. J.; Ditchfield, R.; Pople, J. A. *J. Chem. Phys.* **1972**, *56*, 2257. (d) Francl, M. M.; Pietro, W. J.; Hehre, W. J.; Binkley, J. S.; Gordon, M. S.; Defrees, D. J.; Pople, J. A. *J. Chem. Phys.* **1982**, *77*, 3654. (e) Gordon, M. S. *Chem. Phys. Lett.* **1980**, *76*, 163.

(19) The d-polarization exponents used for basis-A and basis-B are the following: B 0.6; C=N 0.8; Al 0.325; Si 0.395; P 0.55; Ga 0.207; Ge 0.246; As 0.293; those for basis-C are the following: B 0.401; C 0.626; N 0.913; Al 0.325; Si 0.395; P 0.55; Ga 0.141; Ge 2.202; As 0.273.

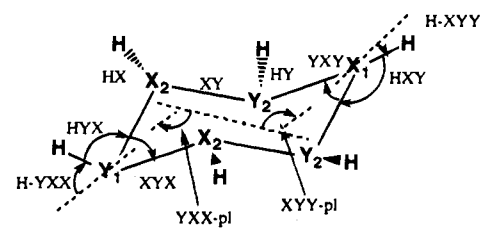
(20) (a) Gordon, M. S.; Nguyen, K. A.; Carroll, M. T. *Polyhedron* **1991**, *10*, 1247. (b) Nguyen, K. A.; Carroll, M. T.; Gordon, M. S. *J. Am. Chem. Soc.* **1991**, *113*, 7924.

(21) (a) Cundari, T. R.; Gordon, M. S. *J. Am. Chem. Soc.* **1992**, *114*, 539. (b) Cundari, T. R.; Gordon, M. S. *Organometallics* **1992**, *11*, 55. (c) Cundari, T. R. *J. Am. Chem. Soc.* **1992**, *114*, 7889.

(22) Frisch, M. J.; Trucks, G. W.; Head-Gordon, M.; Gill, P. M. W.; Wong, M. W.; Foresman, J. B.; Johnson, B. G.; Schlegel, H. B.; Robb, M. A.; Gonzalez, C.; Martin, R. L.; Fox, D. J.; Defrees, D. J.; Baker, J.; Stewart, J. J. P.; Pople, J. A.; GAUSSIAN 92, Gaussian, Inc.: Pittsburgh, PA, 1992.

(23) Krishnan, R.; Binkley, J. S.; Seeger, R.; Pople, J. A. *J. Chem. Phys.* **1980**, *72*, 650.

(24) Binning, R. C., Jr.; Curtiss, L. A. *J. Comput. Chem.* **1990**, *11*, 1206. These bases are augmented with d-polarization functions listed in ref 19 and p-polarization functions for hydrogen (0.75).

Table 1. Geometries of Chair Conformers for  $X_3Y_3H_6$  Compounds<sup>a</sup>


$X_3Y_3H_6$	XY	HX	HY	YXY	XYX	HXY	HYX	XYY-pl <sup>b</sup>	YXX-pl <sup>b</sup>	H-YYY <sup>c</sup>	H-YXX <sup>c</sup>	Hessian <sup>d</sup>
Si <sub>6</sub> H <sub>6</sub>	2.232	1.485		118.8		119.0		161.0		17.8		+
Si <sub>3</sub> Ge <sub>3</sub> H <sub>6</sub>	2.308	1.492	1.543	111.4	118.6	114.4	116.1	143.2	140.6	42.9	30.5	+
Ge <sub>6</sub> H <sub>6</sub>	2.385	1.545		112.5		113.0		133.5		45.2		<i>i</i>
	[2.396]	[1.564]		[111.4]		[112.2]		[130.2]		[47.8]		[+]
B <sub>3</sub> P <sub>3</sub> H <sub>6</sub>	1.910	1.204	1.408	120.4	109.0	119.5	105.9	138.7	143.0	7.6	61.9	+
B <sub>3</sub> As <sub>3</sub> H <sub>6</sub>	2.027	1.192	1.507	121.1	103.4	119.1	100.9	128.8	136.8	8.2	72.2	+
Al <sub>3</sub> P <sub>3</sub> H <sub>6</sub>	2.315	1.584	1.415	117.1	106.8	121.3	103.2	129.6	134.3	5.8	67.4	+
Al <sub>3</sub> As <sub>3</sub> H <sub>6</sub>	2.422	1.583	1.513	119.3	98.8	120.2	97.0	118.9	129.4	6.0	79.2	+
Ga <sub>3</sub> P <sub>3</sub> H <sub>6</sub>	2.312	1.567	1.407	118.6	102.9	120.5	100.5	124.6	132.2	6.2	73.0	+
Ga <sub>3</sub> As <sub>3</sub> H <sub>6</sub>	2.414	1.569	1.513	119.6	97.8	120.0	96.8	117.6	129.0	6.4	79.6	+

<sup>a</sup> The geometries are obtained at the RHF/basis-A level of theory. The values in square brackets are the geometries obtained at the MP2/basis-A level of theory. Bond lengths are in Å, and bond angles are in deg. <sup>b</sup> Plane-plane torsion angles: XYY-pl refers to the torsion angle between the planes formed by  $X_1Y_2Y_2$  and  $Y_2Y_2X_2X_2$ , and YXX-pl refers to the torsion angle between the planes formed by  $Y_1X_2X_2$  and  $Y_2Y_2X_2X_2$ . The dotted lines represent the bisectors of these planes. <sup>c</sup> Bond-plane torsion angles: H-YYY refers to the torsion angle of the bond H-X<sub>1</sub> with respect to the plane  $X_1Y_2Y_2$ . H-YXX refers to the torsion angle of the bond H-Y<sub>1</sub> with respect to the plane  $Y_1X_2X_2$ . <sup>d</sup> A + indicates that the compound is a minimum on the potential energy surface, and *i* indicates a number of imaginary frequency (*i* is a transition state).

order Møller-Plesset perturbation theory (MP2)<sup>25</sup> for both the ECP and all-electron bases.

Bonding in prismanes was analyzed by using localized molecular orbitals (LMO), constructed with the method of Mezey and Pipek.<sup>26</sup> The AIMPAC system of programs<sup>27</sup> was also used to elucidate the nature of the bonding. The density analysis has been discussed in detail elsewhere, and only a few key points will be repeated here. Bond and ring critical points will be of interest in the following discussion. A bond critical point exists between two atoms if there is a "saddle point" in the electron density  $\rho_c$  between the two atoms. At such a point the gradient of the electron density is zero and the hessian of the electron density has one positive eigenvalue along the bond axis. The existence of a bond critical point implies the existence of a bond path (path of maximum electron density passing through the bond critical point), and the two atoms are said to be bonded. The hessian of the electron density at a ring critical point has two positive and one negative eigenvalues, with the density  $\rho_r$  at the ring critical point being smaller than that of all the surrounding bond critical points. The wave functions used for this analysis were obtained with the all-electron basis set (basis-C).

## Results and Discussion

**A. Chair and Boat Conformers.** As has been mentioned previously<sup>6,11,13</sup> many of the planar structures **1** are not minima on the corresponding PES. For the group III-group V analogs only the planar structures containing alternating nitrogen atoms are minima. For the group IV analogs, only those species containing alternating carbon atoms are minima. The only true transition states (with one imaginary frequency) are the planar geometries of Si<sub>6</sub>H<sub>6</sub> and Si<sub>3</sub>Ge<sub>3</sub>H<sub>6</sub>. The remaining planar compounds studied here are third-order saddle points, with three imaginary frequencies. The geometries of conformers **2** (chair) and **3** (boat) are shown in Table 1 and 2, respectively (the supplementary material gives complete cartesian coordinates for each species). The geometries of the benzene-like planar

structures are included in Table 3, adopted from our previous paper.<sup>13</sup> The energy hessian information, indicating whether the compound is a minimum, transition state, or higher-order saddle point, is also included in Tables 1-3.

The normal mode corresponding to the negative eigenvalue of the energy hessian for each of the true transition states (see Table 3), *i.e.* Si<sub>6</sub>H<sub>6</sub> and Si<sub>3</sub>Ge<sub>3</sub>H<sub>6</sub> of structure **1**, is distortion to the chair conformation **2**, and it belongs to the  $a_2''$  representation of  $D_{3h}$  symmetry. The remaining planar structures, namely hexagermabenzene and the ones containing phosphorus and arsenic, are third-order saddle points (Table 3). One of the normal modes,  $a_2''$ , is a distortion to **2** as noted for Si<sub>6</sub>H<sub>6</sub> and Si<sub>3</sub>Ge<sub>3</sub>H<sub>6</sub>. The other two imaginary modes belong to the  $e''$  representation of  $D_{3h}$  and are doubly degenerate distortions to **3**. Therefore, while our main interest in this work is in the structure, stability, and bonding of prismane, we begin with a brief discussion of the chair (**2**) and boat (**3**) conformations.

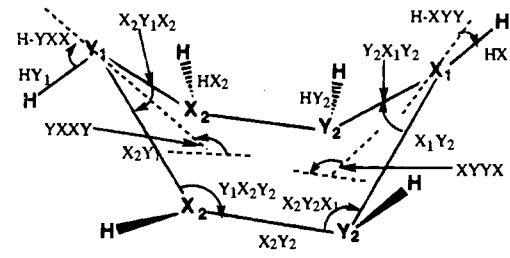
The gross features of the group III-group V chair structures **2** consist of three nearly coplanar X atoms (group III) bonded to Y atoms (group V) in which the bond angles around the Y atoms are somewhat larger than their YH<sub>3</sub> counterparts (as shown in Table 4) to compensate for the cyclization. The sum of the angles around the X atoms is close to 360° in both the group III-group V and the hexasila structure (Table 1). In the case of the boat conformer **3** (Table 2) the X atoms are nearly planar, except for the hexagerma analog, and the angles around the Y atoms deviate considerably from the equilibrium angle of YH<sub>3</sub>. The X-Y bond lengths in **2** and **3** are, in general, longer than those of the corresponding structure **1**.

It is apparent that the phosphorus and arsenic containing compounds do not have good overlap among their  $\pi$ -orbitals, and the deformation of **1** is therefore inevitable.<sup>5,32</sup> These distortions can be understood by examining the inversion barriers of YH<sub>3</sub> where Y is either N, P, or As. The calculated barriers are 6.5, 34.9, and 42.6 kcal/mol, respectively, at the MP2/basis-A/RHF/basis-A level of theory, as shown in Table 4. These barriers are in good agreement with previous *ab initio* calculations.<sup>28</sup> The ammonia inversion barrier is substantially

(25) (a) Carsky, P.; Hess, B. A., Jr.; Schaad, L. J. *J. Comput. Chem.* **1984**, *5*, 280. (b) Møller, C.; Plesset, M. S. *Phys. Rev.* **1934**, *46*, 618.

(26) Pipek, J.; Mezey, P. Z. *J. Chem. Phys.* **1989**, *90*, 4916.

(27) Bader, R. F. W. *Atoms in Molecules—A Quantum Theory*; University of Oxford: Oxford, 1990.

**Table 2.** Geometries of Boat Conformers for  $X_3Y_3H_6$  Compounds<sup>a</sup>


$X_3Y_3H_6$	$X_2Y_2$	$X_1Y_2$	$X_2Y_1$	$HX_1$	$HX_2$	$HY_1$	$HY_2$	$Y_2X_1Y_2$	$X_2Y_1X_2$	$Y_1X_2Y_2$	$X_2Y_2X_1$	$H-YYY^b$	$H-YXX^b$	$YXXY^c$	$YXXY^c$	Hessian <sup>d</sup>
$Ge_6H_6$	2.385	2.385		1.544	1.544			112.5		112.4		45.2		133.3		2i
$B_3P_3H_6$	1.912	1.909	1.892	1.203	1.202	1.404	1.408	117.7	116.7	121.2	110.8	11.5	44.2	134.9	164.9	+
$B_3As_3H_6$	2.038	2.031	2.012	1.203	1.203	1.511	1.516	116.0	110.9	123.2	104.8	11.9	60.0	122.2	157.0	+
$Al_3P_3H_6$	2.319	2.317	2.299	1.583	1.582	1.410	1.416	113.8	117.0	118.8	107.3	8.4	48.7	122.2	159.2	+
$Al_3As_3H_6$	2.447	2.437	2.423	1.591	1.590	1.508	1.516	112.7	105.8	112.4	98.7	7.0	69.0	109.5	146.7	+
$Ga_3P_3H_6$	2.320	2.314	2.301	1.566	1.566	1.403	1.408	113.0	111.8	120.8	104.0	8.5	59.1	117.1	154.2	+
$Ga_3As_3H_6$	2.430	2.416	2.408	1.568	1.570	1.509	1.515	112.4	104.8	123.0	98.7	7.2	70.8	109.5	147.0	+

<sup>a</sup> The geometries are obtained at the RHF/basis-A level of theory. Bond lengths are in Å, and bond angles are in deg. <sup>b</sup> Bond-plane torsion angles: H-YYY refers to the torsion angle of the bond H-X<sub>1</sub> with respect to the plane X<sub>1</sub>Y<sub>2</sub>Y<sub>2</sub>. H-YXX refers to the torsion angle of the bond H-Y<sub>1</sub> with respect to the plane Y<sub>1</sub>X<sub>2</sub>X<sub>2</sub>. The dotted lines represent the bisectors of the planes formed from either X<sub>1</sub>Y<sub>2</sub>Y<sub>2</sub>, Y<sub>1</sub>X<sub>2</sub>X<sub>2</sub>, or X<sub>2</sub>X<sub>2</sub>Y<sub>2</sub>Y<sub>2</sub>. <sup>c</sup> Plane-plane torsion angles: YXXY refers to the torsion angle between the planes formed by X<sub>1</sub>Y<sub>2</sub>Y<sub>2</sub> and Y<sub>2</sub>Y<sub>2</sub>X<sub>2</sub>X<sub>2</sub>, and YXXY refers to the torsion angle between the planes formed by Y<sub>1</sub>X<sub>2</sub>X<sub>2</sub> and Y<sub>2</sub>Y<sub>2</sub>X<sub>2</sub>X<sub>2</sub>. <sup>d</sup> A + indicates that the compound is a minimum, and i indicates a number of imaginary frequency (2i is a second-order saddle point).

**Table 3.** Geometries of  $X_3Y_3H_6$  Inorganic Benzenes<sup>a</sup>

$X_3Y_3H_6$	X-Y	X-H	Y-H	YXY	YXX	Hessian <sup>b</sup>
$C_6H_6^c$	1.406 (1.396)	1.091 (1.083)		120.0 (120.0)		+
$Si_3C_3H_6$	1.766	1.483	1.094	121.3(Si)	118.7(C)	+
$Ge_3C_3H_6$	1.828	1.527	1.080	121.4(Ge)	118.6(C)	+
	[1.845]	[1.540]	[1.097]	[121.0]	[119.0]	[+]
$Si_6H_6$	2.223	1.483		120.0		i
$Si_3Ge_3H_6$	2.262	1.475	1.523	119.2(Si)	120.8(Ge)	i
$Ge_6H_6$	2.306	1.521		120.0		3i
	[2.324]	[1.539]		[120.0]		[3i]
$B_3N_3H_6^d$	1.434	1.209	1.008	117.5	122.5	+
	[1.442]	[1.217]	[1.027]	[117.0]	[123.0]	[+]
	(1.44)	(1.20)	(1.00)	(118)	(121)	
$B_3P_3H_6^e$	1.868	1.198	1.397	116.6	123.4	3i
	(1.84)			(115.)	(124.)	
$B_3As_3H_6$	1.956	1.186	1.482	116.0	124.0	3i
$Al_3N_3H_6^f$	1.787	1.584	1.016	114.2	125.8	+
	(1.78)			(115)	(125)	
$Al_3P_3H_6$	2.275	1.578	1.405	112.8	127.1	3i
$Al_3As_3H_6$	2.359	1.573	1.489	112.4	127.6	3i
$Ga_3N_3H_6$	1.814	1.564	1.006	114.0	126.0	+
$Ga_3P_3H_6$	2.264	1.556	1.393	113.4	126.6	3i
$Ga_3As_3H_6$	2.345	1.554	1.489	112.8	127.2	3i

<sup>a</sup> X refers to the more electropositive elements. XYX and YXY are internal ring angles. Bond lengths are in Å and angles are in deg. The values in parentheses are experimental geometries. The values in square brackets are obtained at the MP2/basis-A level of theory. All other values are obtained at the RHF/basis-A level of theory. <sup>b</sup> A + indicates that the compound is a minimum on the potential energy surface, and i indicates a number of imaginary frequency (i is a transition state and 3i is a third-order saddle point). <sup>c</sup> See ref 28 (p 717). <sup>d</sup> See ref 39 (references therein). <sup>e</sup> See refs 9a-c. <sup>f</sup> See refs 9d,e.

smaller than those for phosphine and arsine, and the H-N-H angle is much larger than H-P-H and H-As-H. This, combined with the weak  $\pi$ -overlap, means that the compounds containing phosphorus and arsenic are expected to have a greater tendency to bend away from planarity. The force constants associated with the "umbrella motion" ( $a_2''$  symmetry) of  $XH_3$ , where X is either B, Al, or Ga, are nearly the same for all three

**Table 4.** Calculated Vibrational Frequencies of  $XH_3$  and  $YH_3$  (X = B, Al, or Ga and Y = N, P, or As)<sup>a</sup>

mode	NH <sub>3</sub>	PH <sub>3</sub>	AsH <sub>3</sub>
	$a_1$	1236	1132
e	1799	1248	1112
$a_1$	3604	2582	2305
e	3748	2585	2316
angle <sup>b</sup>	105.8	95.4	93.7
barrier <sup>c</sup>	6.5	34.9	42.6
imag mode <sup>d</sup> $a_2''$	1002 (5.30)	1249 (17.38)	1273 (21.50)

mode	BH <sub>3</sub>	AlH <sub>3</sub>	GaH <sub>3</sub>
	$a_2''$	1200 (10.54)	758 (8.30)
e'	1260	836	840
$a_1'$	2652	1994	1972
e'	2767	1995	2016

<sup>a</sup> Vibrational frequencies (in  $cm^{-1}$ ) are calculated at the RHF/basis-A level of theory. The values in parentheses are the force constants (in  $mdyn/\text{Å}$ ). <sup>b</sup> The H-Y-H angle. Values are in deg. <sup>c</sup> Inversion barrier (in kcal/mol) is calculated at the MP2/basis-A/RHF/basis-A level of theory. <sup>d</sup> Imaginary frequencies (in  $cm^{-1}$ ) of the planar  $YH_3$ . The values in parentheses are the force constants (in  $mdyn/\text{Å}$ ).

cases. The fact that these force constants, shown in Table 4, are similar and the barriers of inversion are substantially higher in  $PH_3$  and  $AsH_3$  than in  $NH_3$  suggest that distortions away from planarity will occur upon cyclization.

Similar arguments can be used for the group IV benzenes. Methyl radical is a planar molecule; however,  $SiH_3$  and  $GeH_3$  radicals are both pyramidal.<sup>29</sup> Furthermore, the inversion barriers of  $SiH_3$  and  $GeH_3$  are relatively low<sup>30</sup> (5.9 and 5.2 kcal/mol). Also, the  $\pi$ -bond strengths, or the rotational barriers, for the group IV ethylene analogs ( $XH_2=YH_2$ ) for C-C, Si-C, Ge-C, Si-Si, Si-Ge, and Ge-Ge systems are 65.4, 35.6, 32.2, 25.1, 25.7, and 25.4, respectively.<sup>31,32</sup> It can be seen that the ability of carbon to form strong  $\pi$ -bonds and the low inversion

(28) (a) Rauk, A.; Allen, L. C.; Clementi, E. *J. Chem. Phys.* **1970**, *52*, 4133. (b) Moc, J.; Morokuma, K. *Inorg. Chem.* **1994**, *33*, 551. (c) Dixon, D. A.; Arduengo, A. J., III *J. Am. Chem. Soc.* **1987**, *109*, 338.

(29) (a) Morehouse, R. J.; Christiansen, J. J.; Gordy, W. *J. Chem. Phys.* **1966**, *45*, 1751. (b) Jackel, G. S.; Christiansen, J. J.; Gordy, W. *J. Chem. Phys.* **1967**, *47*, 4274.

(30) Moc, J.; Rudzinski, J. M.; Ratajczak, H. *Chem. Phys.* **1992**, *159*, 197.

**Table 5.** Relative Energies of Chair Conformers<sup>a</sup>

X <sub>3</sub> Y <sub>3</sub> H <sub>6</sub>	RHF/RHF/basis-A <sup>b</sup>			MP2/RHF/basis-A <sup>b</sup>		
	basis-A	basis-B	basis-C	basis-A	basis-B	basis-C
Si <sub>6</sub> H <sub>6</sub>	-0.1	-0.0	-0.1	-1.6	-2.2	-3.0
Si <sub>3</sub> Ge <sub>3</sub> H <sub>6</sub>	-3.9	4.2	-3.4	-6.5	1.1	-4.8
Ge <sub>6</sub> H <sub>6</sub> <sup>c</sup>	-15.8	1.9	-4.2	-19.3	-4.0	-10.7
B <sub>3</sub> P <sub>3</sub> H <sub>6</sub>	-9.3	-6.8	-5.7	-1.7	1.0	-0.2
B <sub>3</sub> As <sub>3</sub> H <sub>6</sub>	-22.8	-23.7	-14.2	-9.0	-9.6	-0.7
Al <sub>3</sub> P <sub>3</sub> H <sub>6</sub>	-8.9	-8.5	-8.2	-12.0	-11.1	-13.6
Al <sub>3</sub> As <sub>3</sub> H <sub>6</sub>	-24.0	-14.1	-17.7	-26.6	-16.9	-21.2
Ga <sub>3</sub> P <sub>3</sub> H <sub>6</sub>	-17.7	-24.0	-15.7	-21.8	-26.4	-20.9
Ga <sub>3</sub> As <sub>3</sub> H <sub>6</sub>	-32.6	-30.6	-25.7	-35.4	-32.8	-29.0

<sup>a</sup> The energies (harmonic ZPE's multiplied by 0.89, incorporated) are relative to the planar structures. Values are in kcal/mol. <sup>b</sup> The RHF/RHF/basis-A (or MP2/RHF/basis-A) means that the single-point RHF (or MP2) energy is calculated with the geometries obtained with the RHF/basis-A level of theory. <sup>c</sup> The compound is not a minimum on the PES; it is a transition state (see text).

**Table 6.** Relative Energies of Boat Conformers<sup>a</sup>

X <sub>3</sub> Y <sub>3</sub> H <sub>6</sub>	RHF/RHF/basis-A <sup>b</sup>			MP2/RHF/basis-A <sup>b</sup>		
	basis-A	basis-B	basis-C	basis-A	basis-B	basis-C
Ge <sub>6</sub> H <sub>6</sub> <sup>c</sup>	-0.7	6.2	-4.0	-0.3	3.9	-10.4
B <sub>3</sub> P <sub>3</sub> H <sub>6</sub>	-5.7	-3.8	-2.8	2.3	3.7	3.2
B <sub>3</sub> As <sub>3</sub> H <sub>6</sub>	-13.3	-16.5	-9.9	3.6	-1.6	4.6
Al <sub>3</sub> P <sub>3</sub> H <sub>6</sub>	-6.4	-6.2	-5.9	-8.4	-7.8	-10.2
Al <sub>3</sub> As <sub>3</sub> H <sub>6</sub>	-17.2	-10.8	-14.4	-24.6	-12.5	-16.7
Ga <sub>3</sub> P <sub>3</sub> H <sub>6</sub>	-13.5	-18.7	-12.1	-15.8	-20.0	-15.9
Ga <sub>3</sub> As <sub>3</sub> H <sub>6</sub>	-27.6	-26.6	-21.4	-29.0	-27.8	-23.5

<sup>a</sup> The energies (harmonic ZPE's multiplied by 0.89, incorporated) are relative to the planar structures. Values are in kcal/mol. <sup>b</sup> The RHF/RHF/basis-A (or MP2/RHF/basis-A) means that the single-point RHF (or MP2) energy is calculated with the geometries obtained with the RHF/basis-A level of theory. <sup>c</sup> The compound is not a minimum on the PES; it is a second-order saddle point (see text).

barriers of SiH<sub>3</sub> and GeH<sub>3</sub> contribute to the stability of planar carbon containing benzenes.

Attempts were made to determine if chair or boat conformers exist for the species containing carbon and nitrogen. The geometries were distorted from **1** to either the chair or boat conformations by moving the atoms in the direction of the corresponding normal mode vectors. Subsequent reoptimization returned the structure back to the planar geometry. Similarly, those compounds whose planar structures are transition states were distorted to a boat conformation. Again, they return to the previously determined stationary points on the PES.

The energetics of these conformers with respect to structures **1** are compared in Table 5 for **2** and Table 6 for **3**. Although the B-P benzene analog has three imaginary frequencies, this species with large substituents ([MeBPPH]<sub>3</sub>) was synthesized.<sup>9a-c,f</sup> All basis sets used here predict the B-P chair conformation to be lower than the benzene structure at the RHF level of theory, but there is essentially no difference between these two isomeric forms at the MP2 level of theory. This is also true for hexasilabenzene, as has been reported earlier.<sup>6c,d</sup>

For the chair conformer of hexagermabenzene, there is considerable disagreement in energetics obtained with the three different basis sets used here; at both the RHF and MP2 levels of theory basis-A predicts **2** to be ≈15 kcal/mol lower relative to **1** than does basis-B. The values obtained with basis-C are in between the values obtained with basis-A and basis-B. The two basis sets are in better agreement with each other for the

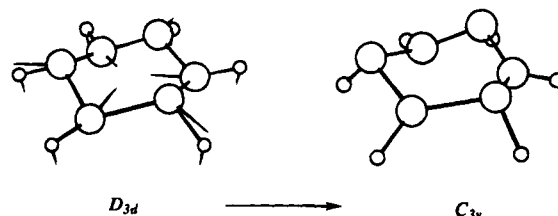


**Figure 1.** Normal mode of Ge-Ge chair conformer and the related minimum. The chair conformer (a transition state) is shown on the left along with its normal mode vectors (64 cm<sup>-1</sup>) corresponding to the negative eigenvalue of the hessian. The structure on the right, which is a minimum at the RHF/basis-A level of theory, is obtained by following the IRC.

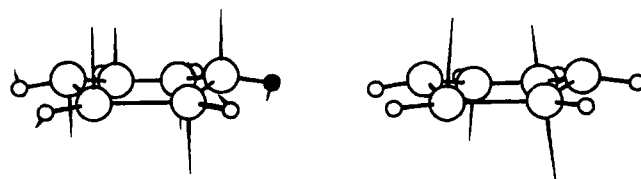


**Figure 2.** Normal modes of Ge-Ge boat conformers. The arrows indicate the normal mode vectors corresponding to the negative eigenvalues (117.1 and 9.5 cm<sup>-1</sup>) of the energy hessian.

Al-P and Ga-As chair structures; both favor the chair conformer by ≥10 kcal/mol. The B-As chair structure exhibits a large correlation effect and basis set effect, with MP2 preferentially favoring the planar structure. The Ga-P and Al-As species are also predicted to strongly favor the chair over the planar structure at all levels of theory. Each of these exhibit a 5–10 kcal/mol basis set effect, but little effect of correlation. In all cases for which both structures are predicted to be minima, **3** is found to be higher in energy than **2** by a few kcal/mol.

The hexagerma analog of **2** is a transition state. The normal mode corresponding to the imaginary vibration (64.3i cm<sup>-1</sup>) is shown in Figure 1, along with the product structure obtained by following the intrinsic reaction coordinate (IRC) using the second-order method of Gonzalez and Schlegel.<sup>33</sup> This structure is a minimum on the PES and lies only 1.7 kcal/mol below **2** at the RHF/basis-A level of theory. However, this structure is calculated to be 8.0 kcal/mol higher in energy than **2** at the MP2/basis-A/RHF/basis-A level of theory. The subsequent MP2/basis-A geometry optimization and the subsequent hessian calculation reveal that the all-germanium chair conformer is in fact a minimum on the PES, and the compound on the right in Figure 1 does not exist. The relative energy of the chair conformer with respect to the planar analog is -18.5 kcal/mol. This is in agreement with the value obtained at the MP2/basis-A/RHF/basis-A level of theory (Table 5).

The boat conformer **3** of the hexagerma analog is a second-order saddle point, even when the double difference technique for obtaining a numerical hessian is used. Figure 2 shows the normal modes associated with the two imaginary frequencies (117.1i and 9.5i cm<sup>-1</sup>). The first mode corresponds to the direction leading to the chair conformer **2**. The second mode assumes a "twisted-boat" conformation. Although it is isoenergetic with **3** (at the MP2 and RHF/basis-A/RHF/basis-A level of theory), the optimized configuration of the twisted-boat is a transition state, having an imaginary frequency of 57.3i cm<sup>-1</sup>. Both forward and reverse directions along the IRC lead to the chair conformer, which is about 16 kcal/mol below **3** at the RHF/basis-A level of theory.

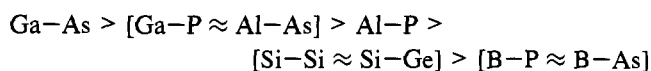
(31) Schmidt, M. W.; Truong, P. N.; Gordon, M. S. *J. Am. Chem. Soc.* **1987**, *109*, 5217.

(32) Windus, T. L.; Gordon, M. S. *J. Am. Chem. Soc.* **1992**, *114*, 9559.

(33) (a) Gonzales, C.; Schlegel, H. B. *J. Phys. Chem.* **1990**, *94*, 5523. (a) Gonzales, C.; Schlegel, H. B. *J. Chem. Phys.* **1991**, *95*, 5853.



For those chair structures which are minima on the respective potential energy surfaces, the following qualitative trend of stabilities is apparent in Table 5, using MP2/basis-C energies:



So, as the participating elements become heavier, distortions from planarity become more favorable, as noted above.

**B. Prismanes.** (i) **Structures and Energetics.** As shown in Scheme 1, the relationship between structure **1** and **4** can be thought of as an intramolecular isomerization. One possible mechanism is an initial cleavage of the  $X_1-Y_1$  bond, followed by breaking the two bonds  $X_2-X_2$  and  $Y_2-X_2$  and forming three  $\pi$ -bonds to obtain **1**.

**Scheme 1**

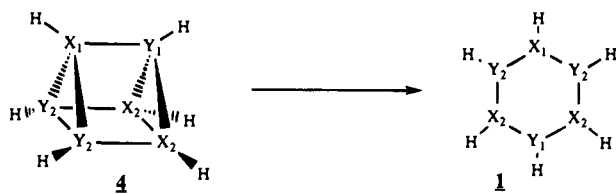
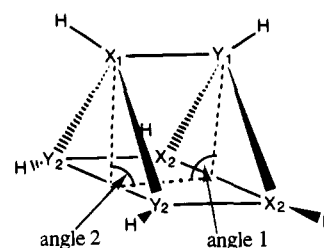


Table 7 shows the bond lengths and the bond angles for prismane analogs (the supplementary material gives complete cartesian coordinates for each species **4**). The bonds between X and Y are substantially longer in **4** than those in the corresponding structures **1**. The differences in the bond distances for hydrogens are small, the largest difference being 0.009 Å. The MP2/basis-A optimized structures for X = Ge, Y = C; X = Y = Ge; and X = B, Y = N give bond lengths that are up to 0.02 Å longer than the SCF structures, since correlation generally introduces some antibonding character. An exception is that the  $X_2Y_2$  bond in the B-N system has been shortened slightly by 0.005 Å. This means that the correlation might favor the stabilization of the two three-membered-ring units in the B-N prismane. However, there are no dramatic structural effects due to correlation.

The only experimentally known geometries of prismane isomers either have an all-carbon backbone (hexamethylprismane) obtained by electron diffraction,<sup>34</sup> an all-silicon frame with six 2,6-diisopropylphenyl groups,<sup>15</sup> or an all-germanium backbone with six  $(\text{Me}_3\text{Si})_2\text{CH}$  groups<sup>14</sup> and six 2,6-diisopropylphenyl groups<sup>15</sup> obtained by X-ray crystallography. The experimental  $X_1-Y_1$  bond lengths in the C-C and Si-Si systems are 1.551 and 2.373 Å, respectively, and the  $X_1-Y_2$  bond lengths are 1.540 and 2.380 Å. These geometries are in good agreement with the calculated values shown in Table 7. The experimental bond lengths for the Ge-Ge prismane with the  $(\text{Me}_3\text{Si})_2\text{CH}$  groups are 2.52 Å for  $X_1-Y_1$  and 2.58 Å for  $X_1-Y_2$ . In the case of 2,6-diisopropylphenyl-substituted Ge-Ge prismane the  $X_1-Y_1$  and  $X_1-Y_2$  bond lengths are 2.468 and 2.503 Å, respectively, so there is considerable variation as a function of substituents. The RHF/basis-A bond lengths for the bonds are both 2.49 Å, much closer to the latter experimental values. Geometry optimization with MP2 has no effect on  $X_1-Y_1$ , but it lengthens  $X_1-Y_2$  by 0.03 Å. The deviation from the MP2 calculated bond lengths is much smaller for the 2,6-diisopropylphenyl-substituted Ge-Ge prismane than in the  $(\text{Me}_3\text{Si})_2\text{CH}$ -substituted compound.

The angle formed by two planes,  $Y_1X_2X_2$  and  $X_2X_2Y_2Y_2$  or  $X_1Y_2Y_2$  and  $X_2X_2Y_2Y_2$  in **4**, is distorted from the ideal angle 90° for the group III-group V prismanes. These angles are

**Table 8.** Torsion Angles of Prismanes<sup>a</sup>



species	X <sub>2</sub>	angle 1	Y <sub>2</sub>	angle 2
B-N	B	85.3	N	87.8
B-P	B	80.4	P	97.1
B-As	B	74.6	As	105.0
Al-N	Al	84.7	N	90.1
Al-P	Al	77.4	P	98.9
Al-As	Al	75.2	As	101.5
Ga-N	Ga	83.4	N	91.3
Ga-P	Ga	77.2	P	99.1
Ga-As	Ga	75.3	As	101.3
C-C		90.0		
C-Si	C	88.7	Si	91.5
C-Ge	C	89.0	Ge	91.8
Si-Si		90.0		
Si-Ge	Si	89.9	Ge	90.1
Ge-Ge		90.0		

<sup>a</sup> Angles are in deg. The angles are formed between the trapezoidal  $X_2X_2Y_2Y_2$  and the triangles  $X_1Y_2Y_2$  and  $Y_1X_2X_2$  of structure **4**. Angle 1 is related to the bending of  $X_2$  atoms, and angle 2 is related to the bending of  $Y_2$  atoms.

summarized in Table 8. The X = Y structures (C, Si, Ge) have, of course, the ideal (undistorted) angle. The most important trend for the mixed compounds is that the distortions in the group III-group V prismanes clearly increase most as the group V elements get heavier. The other distortions are not nearly as large. All of the P and As containing prismanes possess angles about 10° different from the ideal angle. It appears that the large difference in the atomic size *alone* does not explain these distortions. These distortions are closely related to the inversion barriers of  $\text{YH}_3$ , where Y is N, P, or As. As shown in Table 4, the inversion barrier of  $\text{AsH}_3$  is the largest among  $\text{YH}_3$  species. Note also that tetravalency is easily achieved for the  $\text{XH}_3$  (X = B, Al, or Ga) moiety upon accepting an electron pair into its empty p-orbital. Then, it follows that the group III elements are easily distorted and that the arsenic would prefer to assume an angle close to its minimum energy angle, 93.7°, of  $\text{AsH}_3$ . It is consistent among the arsenic containing species (see angle 2 in Table 8) that they possess large distortions. Phosphorus analogs are also strongly distorted. On the other hand, nitrogen containing species prefer to remain close to the ideal angle due to the relatively low inversion barrier. In the case of the group IV species, the angles are all nearly 90.0°. Again the atomic size difference does not play an important role in this distortion. Even for the C-Ge analog that has the largest difference in atomic size, the deviation is only a few degrees.

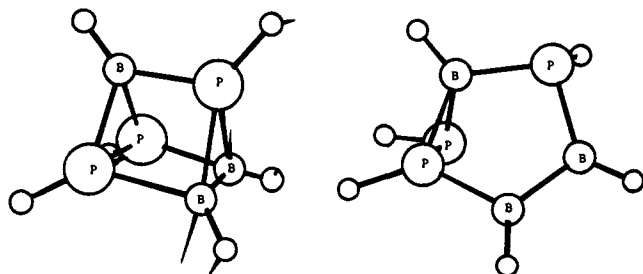
The relative energies of prismanes are compared with the corresponding structures **1** in Table 9. If nitrogen or carbon is present in a molecule, the relative energy becomes high. The B-N prismane is the highest energy species of all, lying 163 kcal/mol above borazine at the MP2/basis-C level of theory. The C-C prismane is also quite energetic (114 kcal/mol above benzene), but as heavier group IV elements are substituted the prismane structure is increasingly stabilized relative to the planar structure. The same trend is observed for the group III-group

(34) Karl, R. R.; Wang, Y. C.; Bauer, S. H. *J. Mol. Struct.* **1975**, *25*, 17.

**Table 9.** Relative Energies of Prismanes<sup>a</sup>

X-Y	RHF//RHF/basis-A <sup>b</sup>			MP2//RHF/basis-A <sup>b</sup>		
	basis-A	basis-B	basis-C	basis-A	basis-B	basis-C
C-C	111.7	123.2	123.6	102.5	116.4	113.9
Si-C	42.7	43.8	48.4	27.6	33.9	35.3
Ge-C	42.8	23.2	40.3	29.3	12.2	27.2
Si-Si	-23.5	-21.0	-15.0	-24.0	-18.3	-13.6
Si-Ge	-12.0	-22.3	-9.8	-11.0	-20.8	-6.4
Ge-Ge	-19.1	-49.4	-9.8	-21.4	-50.1	-11.1
B-N	185.0	185.9	187.1	161.2	162.8	162.6
B-P	93.0	98.2	96.4	70.5	76.2	71.2
B-As	48.9	45.9	59.6	24.9	22.4	33.0
Al-N	102.4	95.5	101.4	88.3	84.8	90.7
Al-P	39.4	41.2	41.4	21.7	23.3	22.8
Al-As	26.3	28.8	31.9	7.9	10.6	12.9
Ga-N	86.1	64.0	82.1	73.4	79.8	96.4
Ga-P	34.8	15.3	37.7	15.5	-2.8	19.1
Ga-As	22.5	4.4	28.5	1.4	-15.3	8.3

<sup>a</sup> The energies (harmonic ZPE, calculated at the RHF/basis-A level of theory, multiplied by 0.89, incorporated) are relative to the planar structures. Values are in kcal/mol. <sup>b</sup> The RHF//RHF/basis-A (or MP2//RHF/basis-A) means that the single-point RHF (or MP2) energy is calculated with the geometries obtained by the RHF/basis-A level of theory.

229 cm<sup>-1</sup>

**Figure 3.** B-P prismane and related minimum. The arrows on the prismane indicate the normal mode vector corresponding to the negative eigenvalue of energy hessian. The molecule on the right is obtained by following IRC.

V species. Indeed, the all-Ge prismane is a low-lying minimum on the Ge<sub>6</sub>H<sub>6</sub> surface. These thermodynamic stabilities in hexagerma- and hexasilaprismane have contributed to the recent syntheses of these compounds.<sup>14,15</sup>

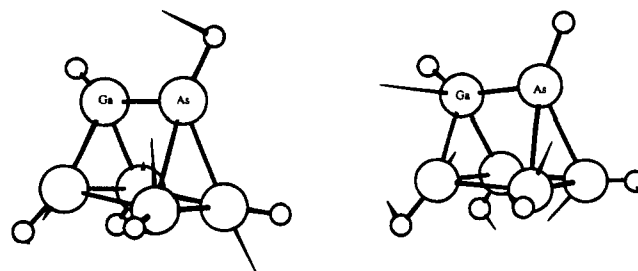
There are significant basis set and correlation effects on the relative stabilities of the prismane structures. With the exception of the Ga-N compound, the general trend is that improvement of the basis set and introduction of correlation both preferentially stabilize the prismane. However, note that for several compounds the ECP basis set A is in much better agreement with the largest basis-C than either is with the intermediate basis-B. This suggests that in those cases in Tables 5 and 6 for which there are serious disagreements between basis sets A and B, the basis-A results are more reliable.

It is difficult to quantify the seemingly unusual stabilities of all-silicon and all-germanium prismanes. The three-membered-ring (cyclopropyl units) of group IV elements, in fact, becomes more strained as the carbon is replaced by silicon or germanium.<sup>6e</sup> Hence it is counter intuitive for the prismanes to have such stabilities. One can, however, speculate about the relative stabilities of  $\pi$ -bonds and the impact on the structures of prismanes. The three  $\pi$ -bonds of all-silicon benzene destabilize the planar conformation relative to benzene itself. As mentioned above, the  $\pi$ -bond strength of ethylene analogs decreases as carbon is replaced with silicon and germanium, and so these

**Table 10.** Electron Density ( $\rho_c$ ) at the Critical Points<sup>a</sup>

	N	B	Al	Ga	
bonds	X <sub>1</sub> Y <sub>1</sub>	0.1691	0.0875	0.1252	
	X <sub>1</sub> Y <sub>2</sub>	0.1302	0.0664	0.0885	
	Y <sub>1</sub> X <sub>2</sub>	0.1255	0.0466		
	X <sub>2</sub> Y <sub>2</sub>	0.0996	0.0557	0.0792	
	Y <sub>2</sub> Y <sub>2</sub>	0.2843	0.2562	0.2639	
rings	X <sub>2</sub> X <sub>2</sub>	0.1597	0.0466	0.0662	
	X <sub>1</sub> Y <sub>2</sub> Y <sub>2</sub>	0.1240	0.0591	0.0752	
	Y <sub>1</sub> X <sub>2</sub> X <sub>2</sub>	0.1254		0.0508	
	P	B	Al	Ga	
bonds	X <sub>1</sub> Y <sub>1</sub>	0.1249	0.0605		0.0802
	X <sub>1</sub> Y <sub>2</sub>	0.1065			0.0584
	Y <sub>1</sub> X <sub>2</sub>	0.0999			0.0491
	X <sub>2</sub> Y <sub>2</sub>	0.0832	0.0412		0.0555
	Y <sub>2</sub> Y <sub>2</sub>	0.1176	0.1084		0.1106
	X <sub>2</sub> X <sub>2</sub>	0.1537	0.0593 <sup>b</sup>		0.0661
rings	X <sub>1</sub> Y <sub>2</sub> Y <sub>2</sub>	0.0894	0.0419		0.0480
	Y <sub>1</sub> X <sub>2</sub> X <sub>2</sub>	0.0951	0.0392		0.0400
	As	B	Al	Ga	
bonds	X <sub>1</sub> Y <sub>1</sub>	0.1283	0.0570		0.0747
	X <sub>1</sub> Y <sub>2</sub>	0.0841			0.0528
	Y <sub>1</sub> X <sub>2</sub>	0.0741			0.0447
	X <sub>2</sub> Y <sub>2</sub>	0.0947	0.0380		0.0511
	Y <sub>2</sub> Y <sub>2</sub>	c	0.0792		0.0804
	X <sub>2</sub> X <sub>2</sub>	0.1650	0.0599 <sup>b</sup>		0.0662
rings	X <sub>1</sub> Y <sub>2</sub> Y <sub>2</sub>	c	0.0388		0.0433
	Y <sub>1</sub> X <sub>2</sub> X <sub>2</sub>	0.0741	0.0370		0.0372
	C	C	Si	Ge	
bonds	X <sub>1</sub> Y <sub>1</sub>	0.2424	0.1145		0.1223
	X <sub>1</sub> Y <sub>2</sub>	0.2437	0.1085		0.1131
	Y <sub>1</sub> X <sub>2</sub>	0.2437	0.1033		0.1107
	X <sub>2</sub> Y <sub>2</sub>	0.2424	0.1134		0.1210
	Y <sub>2</sub> Y <sub>2</sub>	0.2437	0.1993		0.2253
	X <sub>2</sub> X <sub>2</sub>	0.2437			0.0686
rings	X <sub>1</sub> Y <sub>2</sub> Y <sub>2</sub>	0.1968	0.0970		0.0994
	Y <sub>1</sub> X <sub>2</sub> X <sub>2</sub>	0.1968	0.0773		0.0636
	Si	Si	Ge	Ge-Ge	
bonds	X <sub>1</sub> Y <sub>1</sub>	0.0882	0.0820		0.0764
	X <sub>1</sub> Y <sub>2</sub>	0.0866	0.0787		0.0734
	Y <sub>1</sub> X <sub>2</sub>	0.0866	0.0804		0.0734
	X <sub>2</sub> Y <sub>2</sub>	0.0882	0.0820		0.0764
	Y <sub>2</sub> Y <sub>2</sub>	0.0866	0.0882 (Si-Si)		0.0734
	X <sub>2</sub> X <sub>2</sub>	0.0866	0.0722 (Ge-Ge)		0.0734
rings	X <sub>1</sub> Y <sub>2</sub> Y <sub>2</sub>	0.0596	0.0528 (Si-Ge-Ge)		0.0496
	Y <sub>1</sub> X <sub>2</sub> X <sub>2</sub>	0.0596	0.0559 (Ge-Si-Si)		0.0496

<sup>a</sup> Values are in au. The electron density is calculated from the RHF wave function using the basis-C. The empty cell indicates where the critical points were not located. <sup>b</sup> The values obtained have three negative eigenvalues. <sup>c</sup> There is no stationary point on the surface of interest (see Figure 8).

141 cm<sup>-1</sup>49 cm<sup>-1</sup>

**Figure 4.** Ga-As prismane and its normal modes. The arrows on the prismane indicate the normal mode vector corresponding to the negative eigenvalues of energy hessian.

species become more stable as trans-bent species. It is perhaps more advantageous thermodynamically to have only  $\sigma$ -bonds in these heavy group IV molecules.



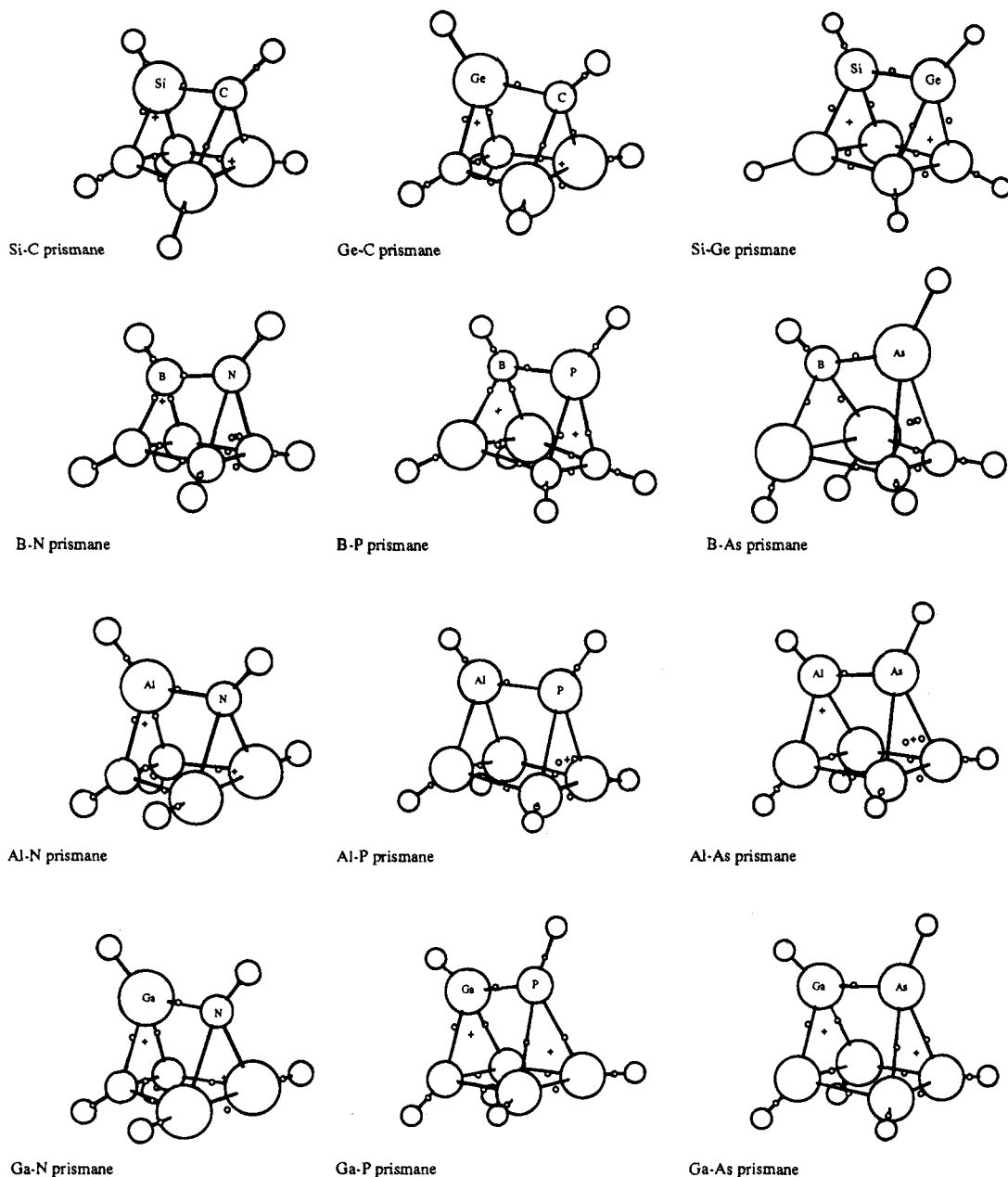


**Figure 5.** Positions of critical points. A smaller circle represents the position of a bond critical point, and a "+" represents the position of a ring critical point. The ring critical points are searched for the rings formed by  $X_1Y_2Y_2$  and  $Y_1X_2X_2$ .

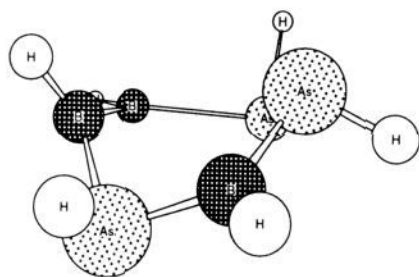
To assess the effect of correlation on predictions of structures and energetics, the geometries of the Ge–C, Ge–Ge, and B–N prismanes were recalculated at the MP2/basis-A level of theory. In each case, the trend in  $\Delta E$  from RHF/basis-A to MP2/basis-A//RHF/basis-A continues when the geometry is reoptimized with correlation included. The relative energies (including ZPE) of the Ge–C, Ge–Ge, and B–N prismanes (**4**) with respect to the planar (**1**) structure, optimized at the MP2/basis-A level of theory, are 18.7, –22.4, and 160.0 kcal/mol, respectively.

As was the case for **1**, not all the prismane analogs are minima on the PES (see the last column of Table 7). The B–P, Al–As, and Ga–P systems are transition states, and the B–As and Ga–As systems are second-order saddle points. The normal mode corresponding to the imaginary vibration of the B–P prismane and its bicyclic product structure determined by following the IRC are shown in Figure 3. A heterolytic cleavage of one of the  $Y_1X_2$  bonds has occurred. This bond is the weaker bond in this prismane, as shown from the value of electron density at the bond critical point in Table 10 (*vide infra*).

Another heterolytic cleavage has occurred at the  $X_2Y_2$  bond, the second weakest bond, to form the product. The product is calculated to be 38.2 kcal/mol more stable than the prismane structure at the MP2/basis-A level of theory. The IRC was not followed for the Al–As and Ga–P systems since they have similar normal modes; however, the product structures were optimized. The relative energies of these species with respect to the corresponding prismanes are –15.3 and –9.2 kcal/mol, respectively, at the same level of theory.

The B–As and Ga–As structures were distorted along the respective normal modes, and the geometries were optimized. As normal modes in both species are similar, only the normal modes for Ga–As prismane are shown in Figure 4. Distortion along either of the two modes shown in Figure 4 and subsequent geometry optimization leads to the structure shown below or to an equivalent enantiomer. The result is an unusual boat-like six-membered ring, and it is a minimum on the PES. The relative energy of the final structure is –13.5 kcal/mol at the MP2/basis-A//RHF/basis-A level of theory. Similarly, the

relative energy of the distorted Ga-As prismane is calculated to be  $-12.8$  kcal/mol, relative to the planar structure at the MP2/basis-A//RHF/basis-A level of theory.



**(ii) Bonding.** The bonding of the prismane structures was analyzed with the atoms-in-molecules method of Bader.<sup>27</sup> Table 10 shows the values of RHF/basis-C electron densities at the critical points.<sup>35</sup> In general, aluminum containing prismanes have smaller electron densities at the bond critical points than do their boron or gallium analogs, and there is a general decrease in  $\rho_c$  upon going from N to P to As for a given group III element.

The positions of the bond critical points illustrate how the electron density is polarized in the bond. This is, then, ostensibly related to the electronegativity of an atom. Figure 5 shows the positions of critical points in heteronuclear analogs of 4. Since electronegative atoms draw the electron density from the neighboring atoms to become electron-rich atoms, the position of the electron density maximum, the bond critical point, is shifted toward the less electronegative of the two atoms. The positions of the bond critical points, denoted by smaller circles, between group III and group V elements lay closer to the group III elements, since these are less electronegative. An exception is the B-As prismane. This is consistent with the equal electronegativities assigned to B and As by Pauling.<sup>36</sup> Although not shown in Figure 5, the homonuclear group IV prismanes have bond critical points equidistant from the two nuclei, and ring critical points are found at the center of the surrounding nuclei (The only ring critical points searched for in this study were within the two rings formed by  $X_1Y_2Y_2$  and  $Y_1X_2X_2$ ). The bond critical points of the bonds  $X_1Y_2$ ,  $Y_1X_2$ ,  $Y_2Y_2$ , and  $X_2X_2$  for the group IV analogs can be found outside the ring or close to the conventionally drawn bonds. However, all of the bond critical points except for the bond  $X_2X_2$  are found on the ring or inside the ring for the group III-group V analogs.

Bond critical points were not found for all apparent bonds, especially if the *effective* atomic sizes are quite different. The effective atomic size can be defined as the relative size of the electron density of an atom in a molecule<sup>27</sup> (see Figure 6, where it may be seen that phosphorus is much larger than aluminum). For example, no bond critical points were found between  $X_1Y_2$ ,  $Y_1X_2$  or  $X_2X_2$  in Al-P prismane (Table 10). However, a substantial amount of electron density exists in the bond region, as shown in Figure 6, even in cases for which a bond critical point was not found (see below).

The localized orbitals plotted in the  $X_1Y_2Y_2$  and  $Y_2X_1X_1$  plane in the B-N prismane are shown in Figure 7a. The valence electrons are all involved in bonding, and all of the X-Y bonds are somewhat polarized toward the nitrogen. The electron-pair donor and acceptor can be readily identified due to the polarization of the localized orbitals, especially those for

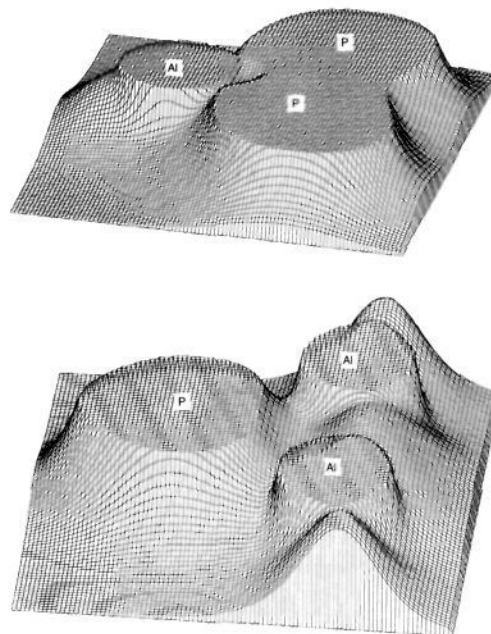


**Figure 6.** Total electron density map of Al-P prismane. The electron density shown here is on the plane of Al-P-P and P-Al-Al. Although the bond critical points for the bonds  $X_1-Y_2$ ,  $Y_1-X_2$ , and  $X_2-X_2$  were not found, the figures show the significant electron density present.

which the electronegativity difference is large. The localized orbitals show that all bonds are strained, since the contour lines bend outside the ring, even though the bond critical point is found close to the center of the ring. There is no apparent anomaly found in the localized orbital corresponding to the Al-Al bond in Figure 7b for Al-P prismane, even though no critical point was found for this bond. As discussed in earlier papers,<sup>20</sup> this illustrates the presence of significant bonding interaction even when there is no bond critical point. Again the electron-pair donor and acceptor are easily identified.

The bond between two As atoms in the B-As analog, Figure 7c, is an electron-deficient multicenter type (the figure in the lower right-hand corner). A substantial amount of boron p-orbital is mixed into this  $\sigma$ -orbital. This is the only compound in this study possessing such bonding. Note that B and As were assigned the same value of the electronegativity by Pauling.<sup>36</sup> The experimental As-As single bond length of 2.372 Å, obtained by X-ray diffraction<sup>37</sup> of  $As_3Co(CO)_3$ , is substantially shorter than the one found here. The total electron density map in the plane of interest is shown in Figure 8. This illustrates that there is a continuous smooth decrease in electron density from the boron center to the midpoint of the two arsenic atoms, in contrast to the saddle point shown in Figure 6.

There seems to be some correlation between the bond strength of a given bond type X-Y and the value of electron density at the bond critical point  $\rho_c(X-Y)$ . The  $\rho_c$  values are plotted in Figure 9 against the elongation of  $X_1-Y_1$ , chosen to be the reference bond for the group III-group V prismanes. A similar plot for the heteronuclear group IV species is shown in Figure 10. For a given group III element in the molecule, the slopes of the curves are similar. Note also that the bond that possesses

(35) We found essentially no difference in the values of electron density and the positions of critical points obtained with basis-B and basis-C.

(36) Pauling, L. *The Nature of The Chemical Bond*, 3rd ed.; Cornell University Press: New York, 1960.

(37) Foust, A. F.; Foster, M. S.; Dahl, L. F. *J. Am. Chem. Soc.* **1969**, *91*, 5631.

(38) Harmony, M. D.; Laurie, V. W.; Kuczowski, R. L.; Scwendeman, R. H.; Lovas, F. J.; Lafferty, W. J.; Maki, A. G. *J. Phys. Chem. Ref. Data* **1979**, *8*, 630.

(39) Boyd, R. J.; Choi, S. C.; Hale, C. C. *Chem. Phys. Lett.* **1984**, *112*, 136.

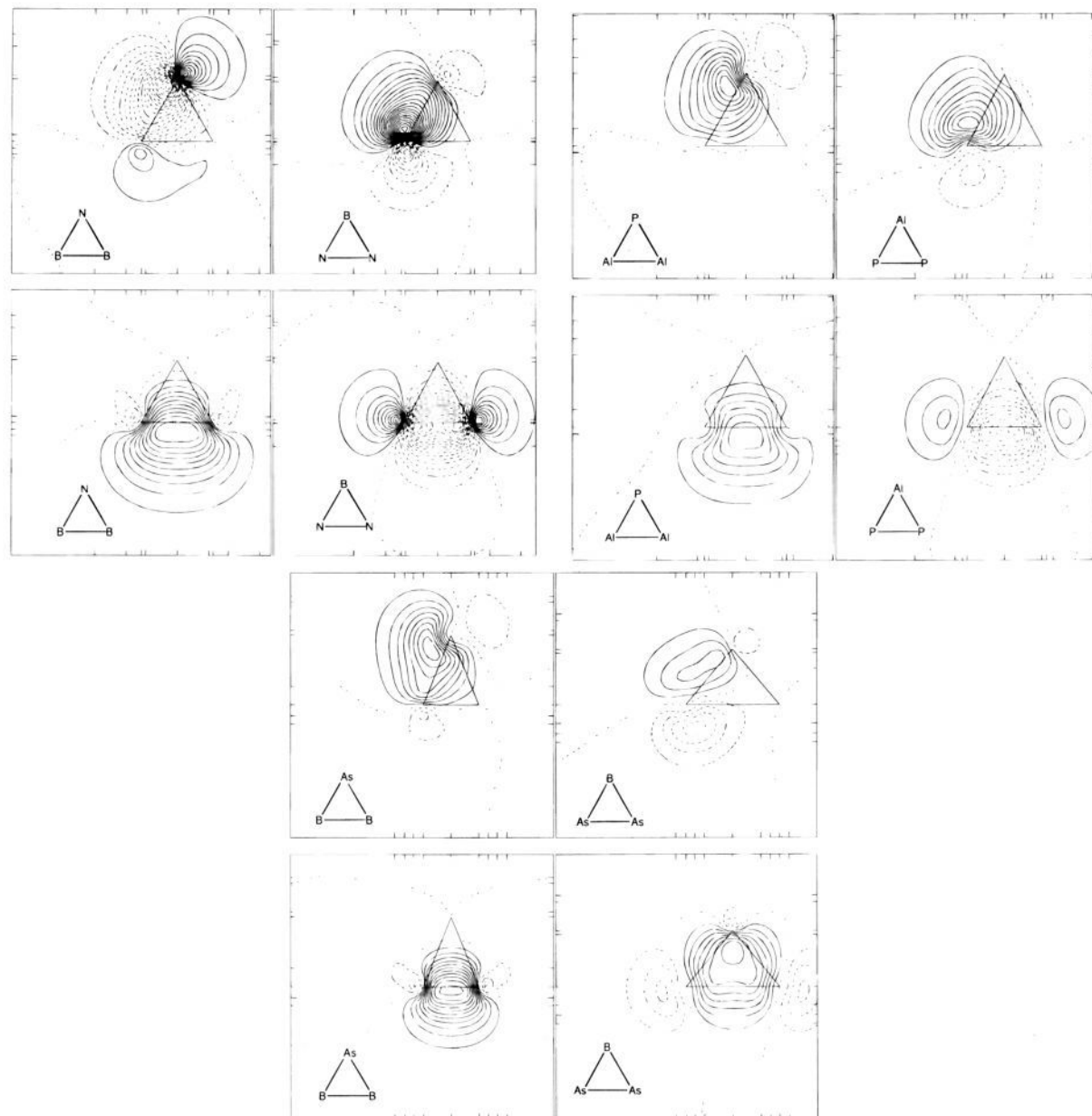


**Figure 7.** Localized orbitals of (a) B–N prismane, (b) Al–P prismane, (c) and B–As prismane (notice the three-center bonding). The successive contours are drawn with  $0.025 \text{ bohr}^{-3/2}$ .

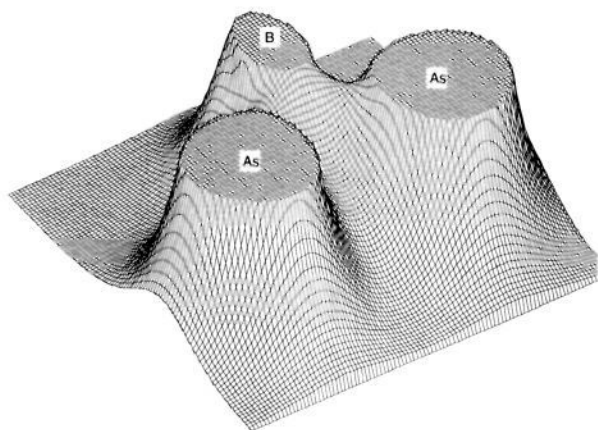


**Figure 8.** Total electron density map of B–As prismane.

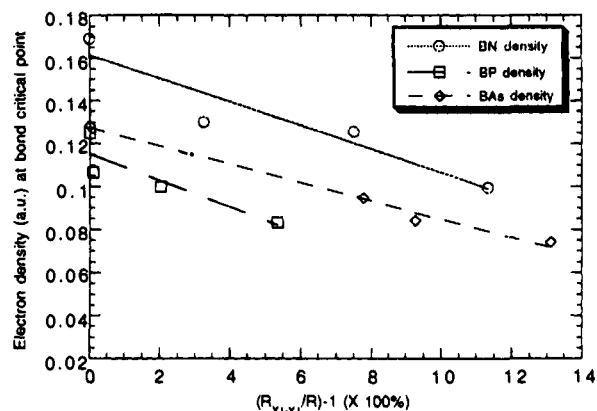
the smallest value of  $\rho_c$  was cleaved in B–P prismane to form the product, shown in Figure 3. The observed trend is consistent

with the structures obtained by distorting the B–As prismane along its imaginary normal modes, in which two bonds with the smallest  $\rho_c$  are cleaved. In general, either the bond  $X_2Y_2$  or  $Y_1X_2$  has the smallest  $\rho_c$  among X–Y bonds. It is interesting to note that the highest  $\rho_c$  values are assigned to the bonds  $Y_2Y_2$  and  $X_1Y_1$ , except for the B–P and B–As analogs. This could imply that the reaction shown in Scheme 1 initiating the reaction by breaking the  $X_1Y_1$  bond, is less likely to occur than the breaking of other bonds with smaller  $\rho_c$  values.

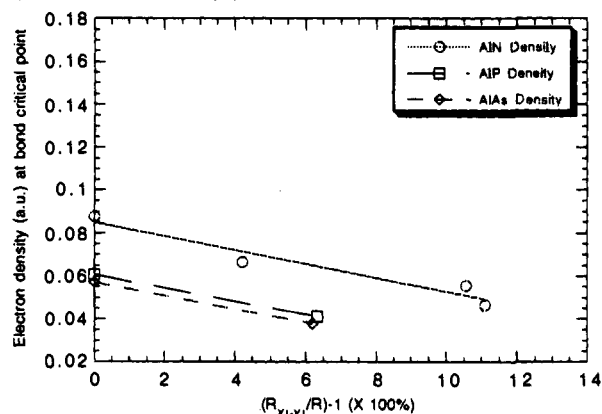
### Summary

In this study we have examined the structures and the stabilities of inorganic prismane analogs, as well as chair and boat conformers of inorganic benzenes. Table 11 summarizes the lowest and highest energy minima in this study. It is interesting to note that, even though theory predicts that the chair conformer of Ga–P benzene is 6 kcal/mol more stable than the boat conformer, the synthesis<sup>10</sup> has yielded a boat

## a) B containing prismanes



## b) Al containing prismanes



## c) Ga containing prismanes

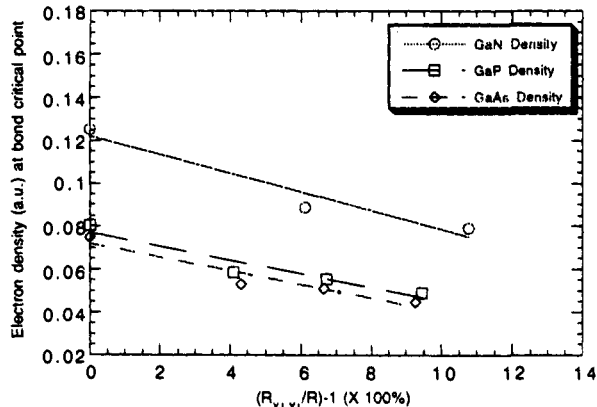


**Figure 9.** Graphs of electron density as a function of X–Y bond elongation.  $(R_{X_1-Y_1}/R) - 1$  represents the percent elongation of a bond, having bond length  $R$ , with respect to the bond  $X_1-Y_1$  for (a) boron containing prismanes, (b) aluminum containing prismanes, and (c) gallium containing prismanes.

structure. This is likely to be due to the more complex substituents in the experimentally studied compounds.

The nitrogen and carbon containing prismanes are stable on the PES, but they are very high in energy, the lowest energy structures being planar when these atoms are present. The B–N system is the highest energy isomer, being 163 kcal/mol above borazine. The hexasila- and hexagermaprismane are the lowest energy prismane isomers found in this study. This thermody-

## Heteronuclear group IV prismanes

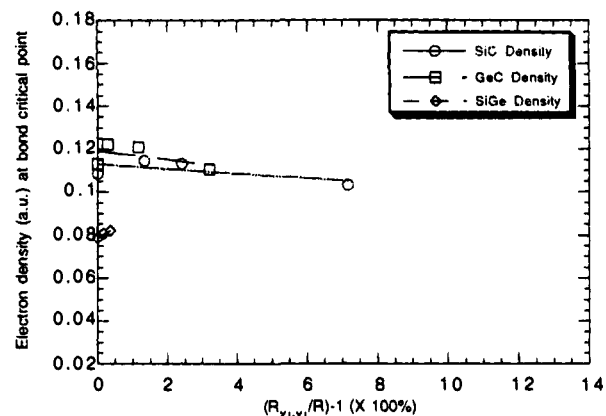


**Figure 10.** Graph of electron density as a function of X–Y bond elongation.  $(R_{X_1-Y_1}/R) - 1$  represents the percent elongation of a bond, having bond length  $R$ , with respect to the bond  $X_1-Y_1$  for heteronuclear group IV prismanes.

**Table 11.** Summary of the Lowest and Highest Energy Isomers<sup>a</sup>

$X_3Y_3H_6$	lowest	highest
C–C	benzene	prismane
Si–C	benzene	prismane
Ge–C	benzene	prismane
Si–Si	prismane	benzene/chair
Si–Ge	chair	benzene
Ge–Ge	prismane	benzene
B–N	benzene	prismane
B–P	chair	$C^b$
B–As	chair	$C^b$
Al–N	benzene	prismane
Al–P	chair	prismane
Al–As	chair	$C^b$
Ga–N	benzene	prismane
Ga–P	chair	$C^b$
Ga–As	chair	boat

<sup>a</sup> The listed isomers are minima on the potential energy surface. <sup>b</sup>  $C^b$  denotes the structure obtained by following the imaginary normal modes. See text.

namic stability contributed to the recent syntheses<sup>15,16</sup> of these compounds. Phosphorus and arsenic prismanes are unstable, except for the Al–P system; they are either transition states or second-order saddle points.

The total electron density analysis together with the localized molecular orbitals give greater insight into stabilities of these molecules. The stability of these molecules can be correlated with the value of electron density of the given bond type at the bond critical points and the shapes of localized orbitals. The localized orbitals show that all of the valence electrons are involved in bonding. The bonds are polarized where electronegativity difference exists for a given bond, and the donor and acceptor are readily identified. The bond  $X_1Y_1$  possesses the highest  $\rho_c$  values and the shortest bond in heteronuclear prismanes, except for the Si–Ge analog. For homonuclear prismanes the  $\rho_c$  values are nearly the same for all bonds between heavy atoms, and in turn the bond lengths are also similar.

**Acknowledgment.** This work was supported in part by grants from the Air Force Office of Scientific Research (92-0226) and the National Science Foundation (CHE-93-13717). The calculations were performed in part on the North Dakota State University IBM ES9000 computer under a joint study

agreement with IBM and in part on an IBM RS6000/530 obtained via a grant to M.S.G. from AFOSR. Some calculations were performed on IBM RS6000/350 computers made available by Iowa State University. Parallel GAMESS was used for some calculations on the CM5 at the Army High Performance Computer Center at the University of Minnesota and on the Intel iPSC/860 at Kirtland Air Force Base. The generous allocation of computer time for calculations of direct MP2 energies on Cray Y-MP and Cray Y-MP C-90 at the Waterway

Experimental Station in Vicksburg, MS, and Cray Y-MP C-90 at the San Diego Supercomputer Center are also acknowledged.

**Supplementary Material Available:** Tables of Cartesian coordinates of optimized geometries of chair, boat, and prismanes (11 pages). This material is contained in many libraries on microfiche, immediately follows this article in the microfilm version of the journal, and can be ordered from the ACS; see any current masthead page for ordering information.